nature cell biology

Regulated ATP release from astrocytes through lysosome exocytosis

Zhijun Zhang[1]*, Gang Chen[1,2]*, Wei Zhou[1,3]*, Aihong Song[1], Tao Xu[4], Qingming Luo[3], Wei Wang[5], Xiao-song Gu[2] and Shumin Duan[1,6]

Release of ATP from astrocytes is required for Ca^{2+} wave propagation among astrocytes[1–3] and for feedback modulation of synaptic functions[2,4,5]. However, the mechanism of ATP release and the source of ATP in astrocytes are still not known. Here we show that incubation of astrocytes with FM dyes leads to selective labelling of lysosomes. Time-lapse confocal imaging of FM dye-labelled fluorescent puncta, together with extracellular quenching and total-internal-reflection fluorescence microscopy (TIRFM), demonstrated directly that extracellular ATP or glutamate induced partial exocytosis of lysosomes, whereas an ischaemic insult with potassium cyanide induced both partial and full exocytosis of these organelles. We found that lysosomes contain abundant ATP, which could be released in a stimulus-dependent manner. Selective lysis of lysosomes abolished both ATP release and Ca^{2+} wave propagation among astrocytes, implicating physiological and pathological functions of regulated lysosome exocytosis in these cells.

Incubation (for more than 1 h) with FM dyes resulted in granule-like fluorescent puncta in cultured astrocytes (Fig. 1). These fluorescent granules were found to be associated with the endocytosis pathway (see Supplementary Information, Fig. S1b–d). To determine the identity of FM-dye-labelled puncta, we immunostained astrocytes with various markers specific for different cellular organelles after incubation or 1 h with AM1-43, a fixable FM1-43 analogue that is largely preserved after immunochemical procedures. We found that immunostaining with specific antibodies against early endosome marker EEA1 or the vesicular glutamate transporters VGluT1 and VGluT2 showed that none of these proteins co-localized with AM1-43 dye. About 3% of cultured astrocytes were immunopositive to anti-secretogranin II, a marker for large dense-core vesicles previously detected in astrocytes[6], but these secretogranin-positive vesicles were not co-localized with AM1-43-stained granules. Thus, these labelled granules are not early endosomes, dense-core secretory vesicles or glutamate-containing vesicles. More than 70% of the AM1-43-stained granules were immunopositive for LAMP1, a specific marker for lysosomes[7] (Fig. 1a–i). In some astrocytes, puncta stained with AM1-43 or LAMP1 were immunopositive for cathepsin D, a secretory lysosomal protease[8], whereas all the cathepsin-D-positive granules showed AM1-43 or LAMP1 staining (Fig. 1e, i). To examine FM labelling of lysosomes in living cells, we transfected astrocytes with two green fluorescent protein (GFP)-linked lysosome markers, namely a membrane protein, CD63, and a small GTPase, Rab-7 (ref. 7). More than 80% of these fluorescent puncta were labelled with FM dyes (Fig. 1f–i). Treatment of cultures with glycylphenylalanine 2-naphthylamide (GPN; 200 μM), a substrate of the lysosomal exopeptidase cathepsin C that selectively induces lysosome osmodialysis[9], largely prevented the appearance of labelled puncta after incubation with FM2-10 but did not affect mitochondrial staining by MitoTracker Red (Fig. 1j–l). Examination of photoconverted FM1-43 in cultured astrocytes by electron microscopy showed electron-dense precipitates in organelles with typical lysosome morphology (Supplementary Information, Fig. S1g). Thus, prolonged incubation of astrocytes with FM dyes selectively labels lysosomes.

Further studies showed that these FM-labelled lysosomes can undergo regulated exocytosis. Application of ATP or glutamate (both at 1 mM) for 7 min induced a 9% or 23% decrease in the fluorescence intensity of puncta labelled with FM1-43 (Fig. 2a, g) and FM2-10 (Fig. 2b, g), respectively. The partial dissociation of the dyes from the lysosome membrane suggests that ATP or glutamate may have induced a brief opening of a fusion pore ('kiss-and-run'), rather than a full fusion of the lysosome with the plasma membrane. This idea is supported by the finding that the same concentration of ATP induced a greater extent of destaining of FM2-10, which has faster dissociation kinetics than FM1-43 (ref. 10). Because FM2-10 and FM1-43 may have labelled different vesicle pools[11],

[1]Institute of Neuroscience and Key Laboratory of Neurobiology, Shanghai Institutes for Biological Sciences, Chinese Academy of Sciences, Shanghai 200031, China. [2]Jiangsu Key Laboratory of Neuroregeneration, Nantong University, Nantong, Jiangsu, 226001, China. [3]Britton Chance Center for Biomedical Photonics, Wuhan National Laboratory for Optoelectronics, Huazhong University of Science & Technology, Wuhan, 430074, China. [4]National Laboratory of Biomacromolecules, Institute of Biophysics, Chinese Academy of Sciences, Beijing, 100101, China. [5]Department of Neurology, Tongji Hospital, Tongji Medical Scool, Huazhong University of Science and Technology, Wuhan, 430030, China.
[6]Correspondence should be addressed to S.D. (e-mail: shumin@ion.ac.cn)
*These authors contributed equally to this work.

Received 26 April 2007; accepted 21 June 2007; published online 8 July 2007; DOI: 10.1038/ncb1620

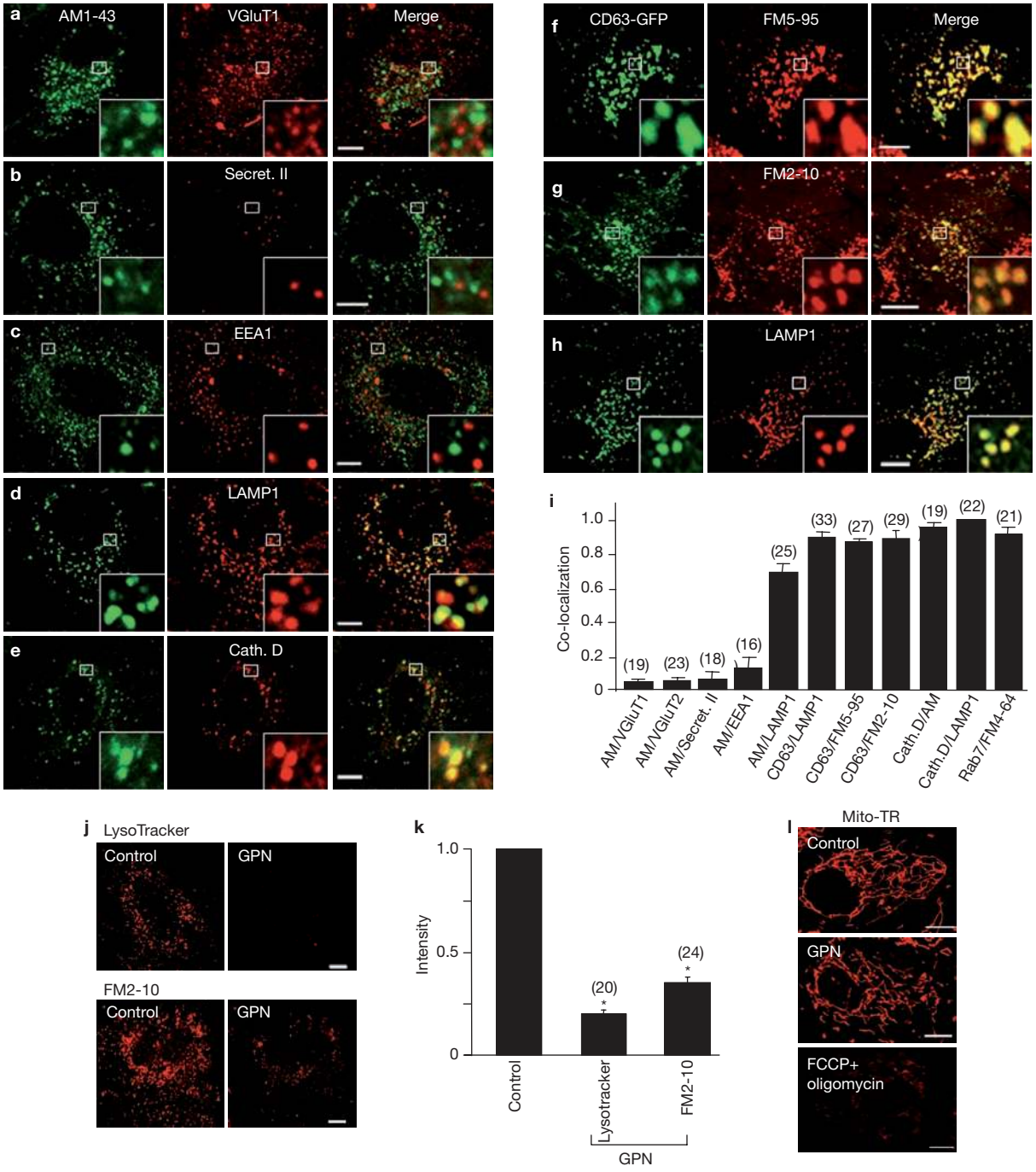

Figure 1 Confocal images showing that prolonged loading of cultured astrocytes with FM dyes specifically labels lysosomes. (**a**–**e**) Astrocytes loaded with AM1-43 (AM, green) were immunostained with different markers (red). Right: overlay of the two fluorescence signals. Secret. II, secretogranin II; Cath. D, cathepsin D. (**f**–**h**) Astrocytes were transfected with GFP-linked CD63 (green), a lysosome membrane marker, before being loaded with FM dyes or immunostained with LAMP1 (red). The boxed areas in **a**–**h** are shown at a higher magnification in the insets. Scale bars, 10 μm (2.2 μm for enlarged images). (**i**) Summary of the co-localization of AM/FM dyes with various markers. The fraction of AM/FM or CD63–GFP puncta showing co-localization of the marker are plotted, for all markers shown in **a**–**h**. The number above each column refers to the total number of cells examined for each condition. Error bars indicate s.e.m. (**j**) Images of puncta labelled by the lysosome tracer LysoTracker or by FM2-10 before (left) and after (right) treatment with 200 μM GPN for 15 min. (**k**) Averaged fluorescence intensity of the puncta labelled by lysotracker or FM2-10 after treatment with GPN, as shown in **i**. Data were normalized to the average fluorescence intensity of the puncta measured before GPN treatment in the same field (control). The number above each column refers to the number of cells examined. Error bars indicate s.e.m. (asterisk, $P < 0.01$ compared with the control; Student's *t*-test). (**l**) Treatment with GPN (middle) did not affect mitochondrial structure revealed by mitochondria tracer (Mito-TR). In contrast, disruption of mitochondria by its specific toxin *p*-trifluoromethoxyphenylhydrazone (FCCP, 1 μM) and oligomycin (10 μM) largely prevented labelling with Mito-TR (bottom).

we further tested the idea of 'kiss-and-run' fusion of FM1-43-labelled lysosomes by using a membrane-impermeant fluorescence quencher bromophenol blue (BPB; ref. 12). Bath application of 1 mM BPB by itself had no effect on the fluorescence intensity of FM1-43-labelled puncta. However, application of 1 mM ATP in the presence of BPB induced a destaining of FM1-43-labelled puncta to an extent (30%) significantly larger than that induced in the absence of BPB (9%), which is consistent with the notion that BPB diffused through the fusion pore during the 'kiss-and-run' process had quenched the FM fluorescence on the inner leaflet of the lysosome membrane (Fig. 2c, g). It is unlikely that the BPB effect was due to its uptake into the endocytic pathway, because the same effect was observed in the presence of the endocytosis inhibitor monodansylcadaverine MDC (data not shown). Furthermore, when astrocytes were incubated with FM1-43 together with BPB for 1 h, subsequent application of ATP induced an increase rather than decrease in FM1-43 fluorescence (Fig. 2d), which is consistent with the dequenching of FM1-43 fluorescence as BPB diffused out of the fluid phase of the lumen before the dissociation of FM1-43 from the lysosomal membrane. Taken together, these results strongly support the notion of 'kiss-and-run' exocytosis of lysosomes induced by ATP and glutamate.

Leakage of lysosome enzymes has been observed during ischaemia[13]. To examine whether lysosomes undergo exocytosis under such pathological conditions, we treated astrocyte cultures with potassium cyanide (KCN), an inhibitor of oxidative phosphorylation that has been used in culture models for inducing chemical hypoxia[14]. We found that 4 mM KCN induced marked destaining of the FM dye-labelled puncta within a few minutes (Fig. 2e–g). For the number of puncta exhibiting different percentages of destaining of FM2-10, we found a single peak at about 20% for ATP-induced destaining, but two peaks at 20% and 100% for KCN-induced destaining (Fig. 2h). Thus, unlike ATP-induced or glutamate-induced lysosome exocytosis, KCN induced both partial and full lysosome exocytosis. Surface staining with LAMP1, an indication of the fusion of lysosomal membranes with the plasmalemma[15], was low in control or ATP-treated cultures but was greatly elevated by treatment with KCN (Supplementary Information, Fig. S1e, f). By using astrocytes transfected with CD63 tagged with green fluorescent protein (CD63–GFP), we were able to observe lysosome exocytosis directly in living cells. After treatment with KCN, the fluorescence of FM2-10-labelled puncta either decreased or disappeared, reflecting partial or full lysosome exocytosis (see Supplementary Information, Fig. S2c d and Movie 1). When the cells were fixed afterwards for immunostaining with anti-LAMP1, we found that most vesicles that were destained either partly or fully during ATP or KCN treatment were LAMP1 positive (Supplementary Information, Fig. S2a, b). Taken together, these results indicate that ATP induces partial exocytosis, whereas KCN induces both complete and partial exocytosis of lysosomes.

How is lysosome exocytosis regulated? Both ATP and KCN treatments induced an elevation of cytoplasmic Ca^{2+} ($[Ca^{2+}]_i$) (Fig. 3a, c). Loading cultures with the membrane-permeable Ca^{2+} chelator BAPTA-AM (bis-(*o*-aminophenoxy)ethane-*N*,*N*,*N*′,*N*′-tetra-acetic acid acetoxymethyl ester), which buffers $[Ca^{2+}]_i$ at a low level, prevented the ATP- or KCN-induced destaining of the FM2-10-labelled puncta. Furthermore, treatment of the culture with the Ca^{2+} ionophore ionomycin induced a more significant destaining of FM2-10-labelled puncta than that induced by ATP or glutamate, presumably because of a higher and more persistent $[Ca^{2+}]_i$ elevation induced by ionomycin (Fig. 3a–c). Thus, Ca^{2+} is both necessary and sufficient for lysosome exocytosis.

The process of lysosome exocytosis was further examined with total-internal-reflection fluorescence microscopy (TIRFM), which allowed us to monitor a subpopulation of FM2-10-labelled puncta near the plasma membrane in contact with the culture substrate (Fig. 3d). Perfusion of ATP induced an initial slight increase followed by a gradual decline of the puncta fluorescence, suggesting the movement of the pre-docked lysosomes towards the substrate and the subsequent partial destaining of the FM dye (Fig. 3e, h, and Supplementary Information, Fig. S3e, f and Movie 2). Perfusion of KCN led to two patterns of changes in fluorescence in the 'docked' puncta at the plasma membrane: some puncta showed fluorescence changes similar to that induced by ATP, whereas a substantial fraction of the puncta showed a marked transient increase followed by a complete disappearance of the FM fluorescence (Fig. 3e, g, and Supplementary Information, Fig. S3 and Movies 2 and 3). In addition, treatment with KCN induced a population of 'new' puncta (Fig. 3e–g and Supplementary Information Movie 3), which may correspond to lysosomes that were recruited from deep cytoplasmic regions towards the plasma membrane. These new puncta showed similar patterns of fluorescence changes as those found for pre-docked puncta (old puncta; Fig. 3g). Finally, we also observed a decrease in the mobility of lysosomes after treatment with ATP or KCN (Fig. 3i, and Supplementary Information, Movie 3), suggesting an increased docking of mobile lysosomes in the vicinity of the plasma membrane[16]. These TIRFM results fully support the notion of differential modes of lysosome exocytosis induced by ATP and by KCN.

Both microtubule-based kinesin and actin-based myosin are involved in the vesicle recruitment for Ca^{2+}-regulated exocytosis that mediates membrane resealing[7]. It is possible that higher and/or more sustained $[Ca^{2+}]_i$ elevation, which can be induced by KCN but not by ATP (Fig. 3a, c), is required for initiating the long-range trafficking and full exocytosis of lysosomes. Calcium release from lysosomes has been reported to be important in elevating $[Ca^{2+}]_i$ and in mediating Ca^{2+} wave propagation in astrocytes[17]. Depletion of intracellular ATP by KCN may induce Ca^{2+} release from lysosomes as a result of the decreased activity of Ca^{2+} pumps in the lysosome membrane. This microdomain Ca^{2+} elevation surrounding the lysosome may be more efficient in triggering the trafficking and full exocytosis of the lysosome than the 'global' $[Ca^{2+}]_i$ elevation induced by ATP. Treatment with KCN, but not with ATP or glutamate, may also induce more complete disruption of the cortical actin cytoskeleton, enabling efficient docking and complete fusion of lysosomes with the plasma membrane.

Exocytosis of astrocyte lysosomes may result in the secretion of lysosomal enzymes as well as other signalling molecules. It is known that astrocytes release glutamate[2,18], but glutamate vesicular transporters VGluT1 and VGluT2 expressed in cultured astrocytes did not co-localize with AM1-43-labelled puncta (Fig. 1a, i), and anti-glutamate immuno-positive puncta, found only in some astrocytes, were also not co-localized with the lysosome marker LAMP1 (Fig. 4a, d). The 'kiss-and-run' exocytosis of the FM dye-labelled vesicles in cultured astrocytes has been implicated in glutamate release[18], although the identity of these vesicles is unknown. It is possible that short-term (of the order of minutes) incubation with the FM dye used by Chen *et al.*[18] labelled a different population of vesicles from those labelled by prolonged (of the order of hours) incubation used in the present study. Nevertheless, it is possible that the level of glutamate in the lysosome is close to that in the cytosol and that no difference was detected by

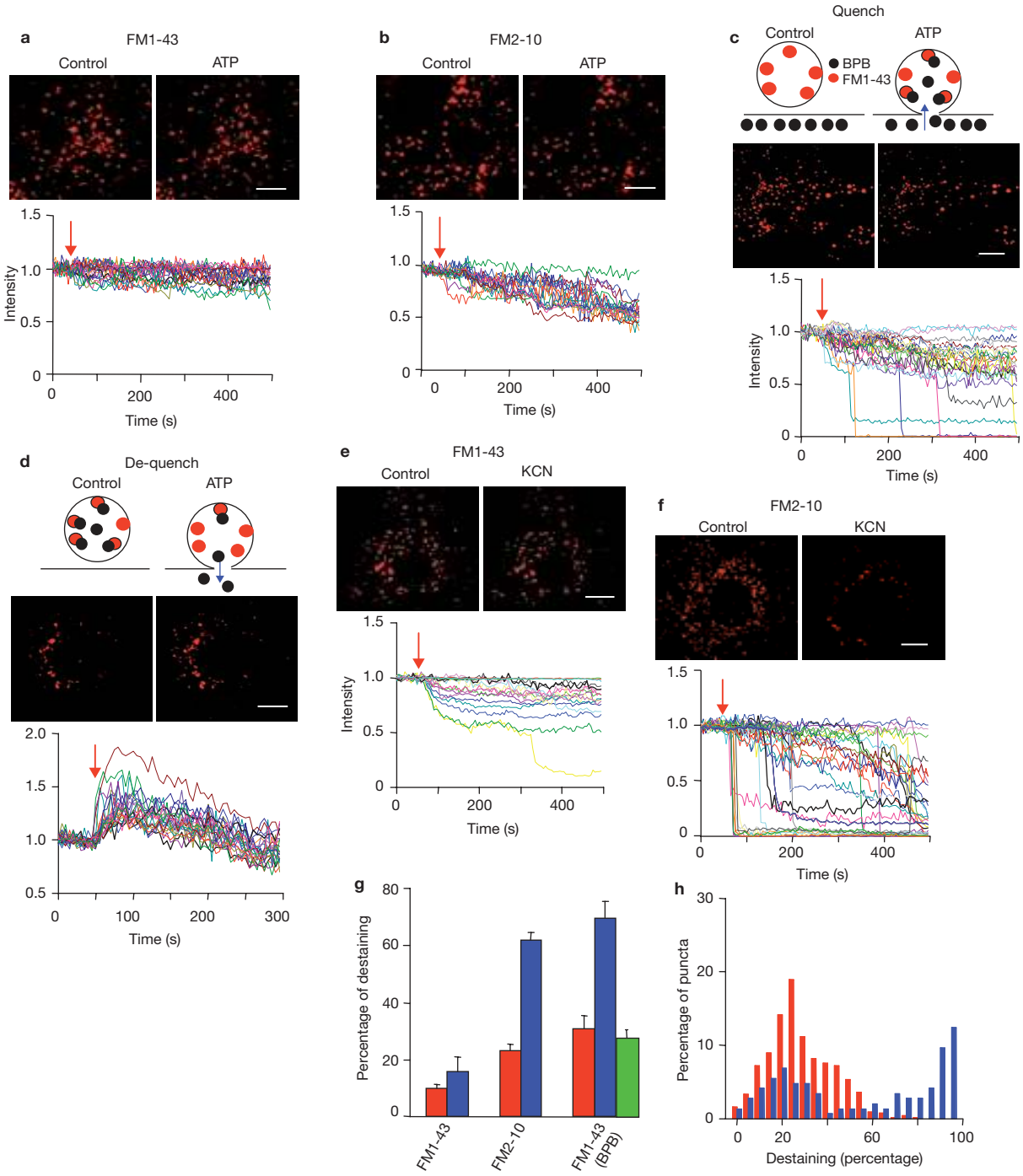

Figure 2 Destaining of the FM dye-labelled puncta in astrocytes by ATP and KCN. (**a**, **b**) Top: example images of puncta labelled by FM1-43 **(a)** and FM2-10 **(b)** before (control) and after perfusion with ATP for 7 min. Bottom: time course of ATP-induced destaining, normalized by that obtained before ATP application (marked by the arrow), for 24 randomly sampled puncta. Each line represents a single punctum. (**c**) ATP-induced destaining of FM1-43 in the presence of 1 mM BPB. Top: schematic illustration showing ATP-induced transient lysosome fusion with the plasmalemma, allowing BPB entering the lysosome to quench FM1-43 fluorescence. Middle: example images of the FM1-43-labelled puncta before (control) and after 7 min perfusion with ATP. Bottom: ATP-induced FM1-43 destaining in the presence of BPB. (**d**) ATP-induced destaining of FM1-43-labelled puncta, which were loaded simultaneously with BPB. Top: schematic illustration showing ATP-induced transient lysosome fusion with the plasmalemma allowing preloaded BPB, but not FM1-43, to diffuse out of the lysosome, leading to a transient increase (de-quenching) of the FM1-43 fluorescence. Middle: example images of puncta loaded simultaneously with FM1-43 and BPB before (control) and after perfusion with ATP for 7 min. Bottom: ATP-induced destaining of 26 randomly sampled puncta preloaded with FM1-43 and BPB. (**e**, **f**) Top: example images of puncta labelled with FM1-43 (**e**) and FM2-10 (**f**) before (control) and after perfusion with 4 mM KCN for 7 min. Bottom: time course of ken-induced destaining in 27 randomly sampled puncta. Data are presented in the same manner as in **a** and **b**. (**g**) Average percentage destaining of puncta labelled with FM1-43 or FM2-10 after 400–500 s of perfusion with ATP (red; $n > 200$ puncta from eight experiments for each dye), glutamate (green; $n > 200$ puncta from seven experiments) or KCN (blue; $n > 300$ puncta from nine experiments). Error bars indicate s.e.m. (**h**) Percentage of the FM2-10-labelled puncta exhibiting different degrees of destaining induced by ATP (red) and KCN (blue). For ATP (1 mM), $n = 1020$ puncta from 12 cells, and for KCN (4 mM), $n = 795$ puncta from 9 cells. Scale bars in **a**–**f**, 10 μm.

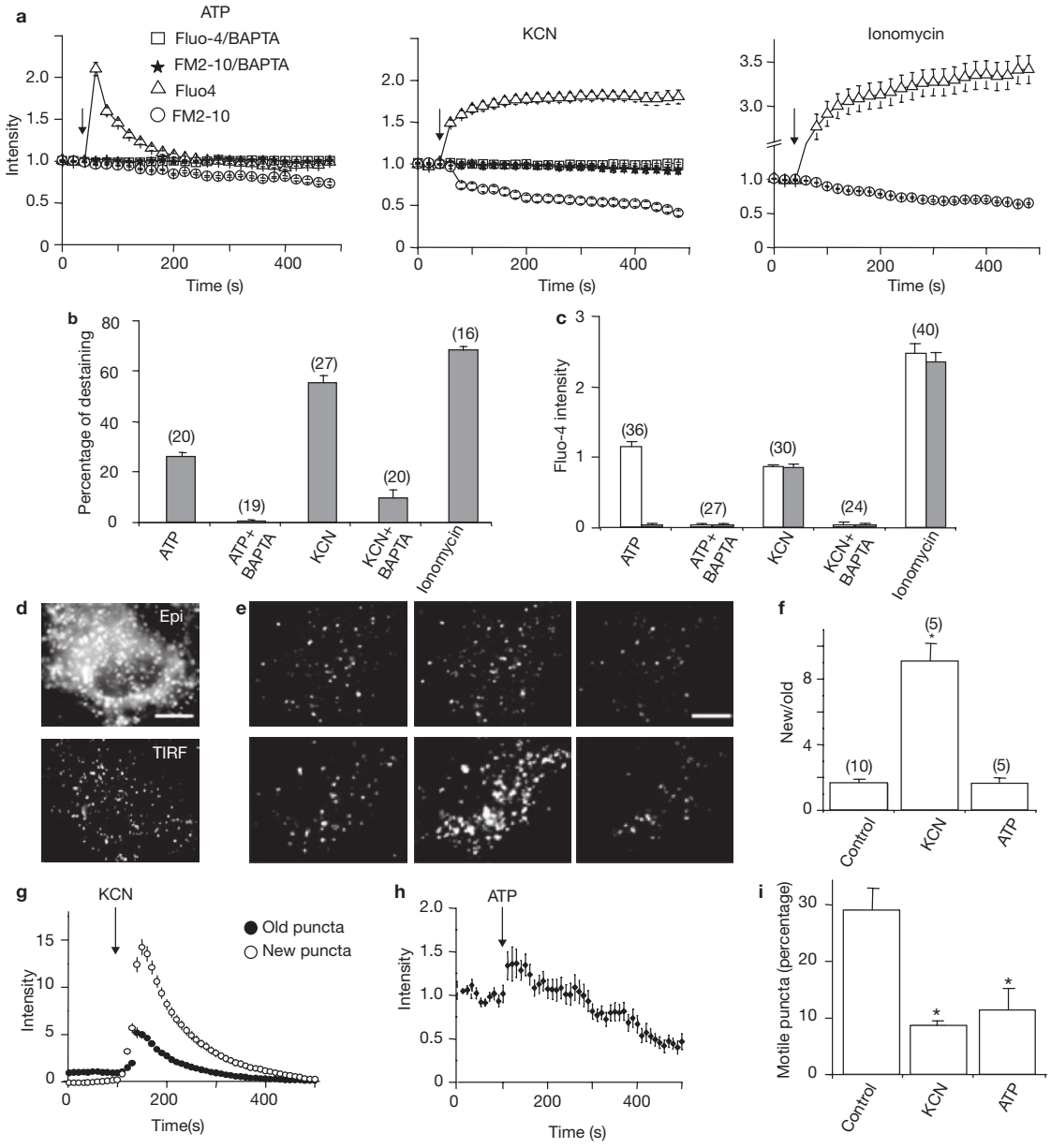

Figure 3 Ca^{2+} dependence and TIRFM imaging of lysosome exocytosis in astrocytes. (**a**) Changes in the fluorescence signals of FM2-10-labelled puncta and cytoplasmic Fluo-4 AM induced by perfusion with ATP, KCN and ionomycin, with or without preloading of BAPTA-AM. Data are normalized to the average fluorescence intensity measured during 50 s (control period) before the onset of drug perfusion (marked by the arrow). (**b**) Percentage of destaining of FM2-10 after perfusion with ATP or KCN for 350–450 s under the conditions shown in **a**. The number above each column refers to the number of cells examined. Error bars indicate s.e.m. (**c**) Average changes in intensity of Fluo-4 AM fluorescence during perfusion with ATP or KCN for 0–50 s (transient phase; open columns) and 350–450 s (sustained phase; filled columns), normalized to the Fluo-4 signal during the 50 s before perfusion for each cell, under the conditions shown in **a**. The number above each column refers to the total number of cells examined. Error bars indicate s.e.m. (**d**) Image of an astrocyte under epifluorescence confocal microscopy and TIRFM. Scale bar, 10 μm. (**e**) TIRFM of the FM2-10-labelled puncta before (left) and after 50 s (middle) and 300 s (right) of perfusion with 1 mM ATP (top) or 4 mM KCN (bottom; see also Supplementary Information, Movie 3). Scale bar, 10 μm. (**f**) Ratio of the new to old puncta detected after perfusion with ATP and KCN for 200 s, compared with untreated controls, from data similar to that shown in **e**. The number above each column refers to the total number of experiments for each condition. (**g**, **h**) Averaged FM2-10 destaining induced by KCN and ATP as shown in **e**. $n = 82$ and 402 puncta were examined for the old and new puncta in **g** and 164 puncta were examined in **h**. Data are normalized to the average fluorescence intensity obtained during the 0–100 s before perfusion with KCN or ATP for each punctum. (**i**) Decrease in the percentage of motile FM2-10-labelled puncta induced by ATP and KCN. Puncta that appeared or disappeared from the evanescent field, or moved a distance of more than 1 μm within the evanescent field during the 500-s sampling period, were classified as motile. Error bars indicate s.e.m. (asterisk, $P < 0.01$ compared with the control group; Student's *t*-test).

the immunostaining method. Because of their large size, exocytosis of lysosomes may still result in a considerable amount of glutamate release even if the lysosome contains a low level of glutamate.

In contrast to glutamate, we obtained clear evidence that lysosomes contain ATP, another important signalling molecule for astrocytes[1–5]. Incubation of cultures with Mant-ATP, a fluorescent nucleotide analogue

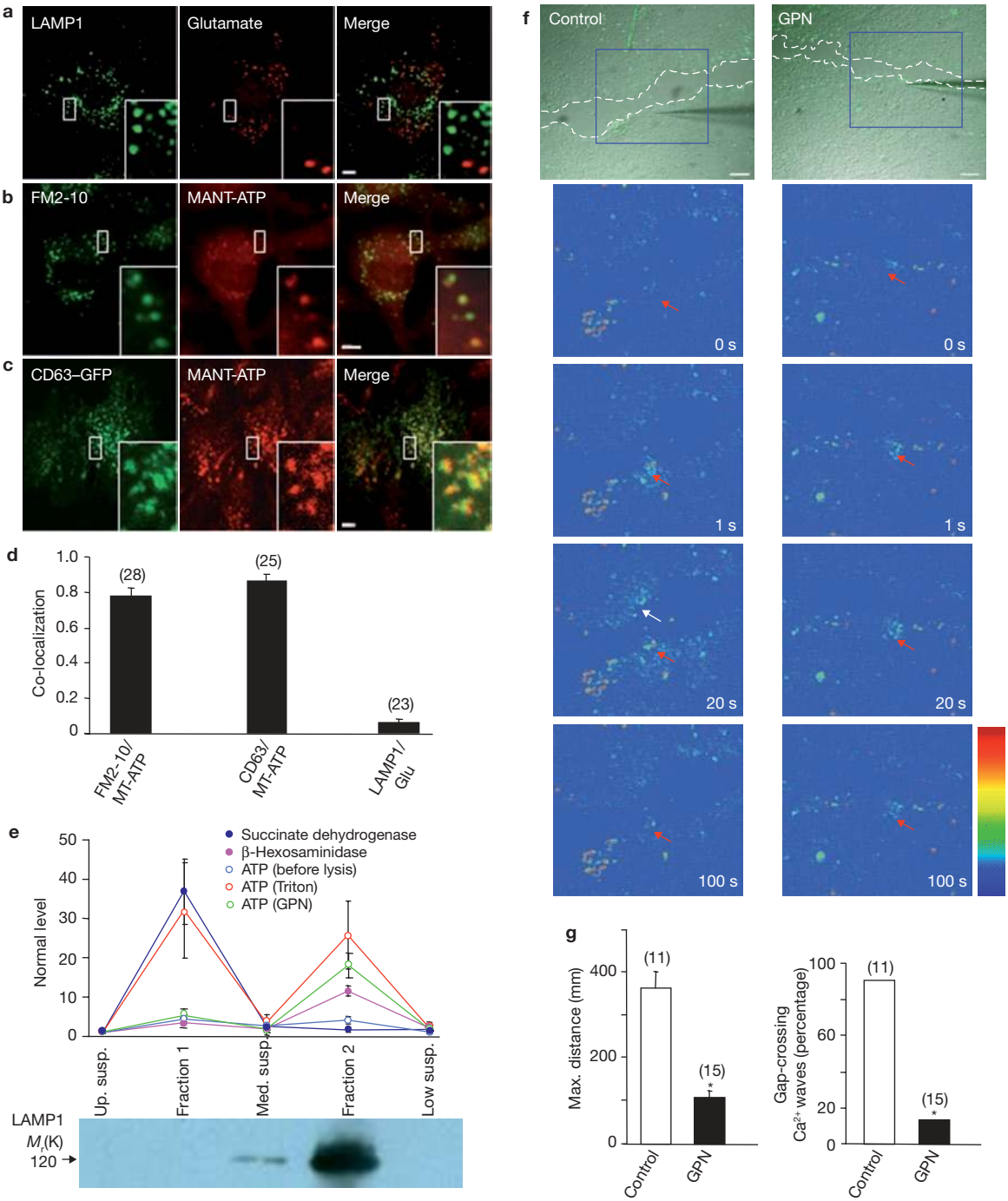

Figure 4 Lysosomes in astrocytes contain abundant ATP. (**a**) LAMP1-positive puncta (green) do not overlap with those immunostained with anti-glutamate (red). (**b**) FM2-10-labelled puncta (green) show accumulation of MANT-ATP (red). (**c**) Puncta labelled by CD63–GFP (green) show accumulation of MANT-ATP (red). Scale bars, 20 μm (2.5 μm for enlarged images). (**d**) Summary of the co-localization of MANT-ATP with FM2-10 or CD63–GFP. The fraction of puncta labelled with FM2-10 or CD63–GFP that accumulated MANT-ATP are plotted, together with data on the fraction of LAMP1-immunopositive puncta that also showed immunostaining for glutamate. The number above each column refers to the total number of cells examined. Error bars indicate s.e.m. (**e**) Top: Relative levels of ATP, the mitochondrial enzyme succinate dehydrogenase and the lysosomal enzyme β-hexosaminidase in various subcellular fractions separated by centrifugation and Percoll gradients (see Supplementary Methods). Data are normalized to the value obtained in the fraction of the upper suspension (up. susp.) from each experiment (n = 7). Med. and low susp., medium and lower suspensions, respectively. Bottom: Example of a western blot with anti-LAMP1 antibodies for different subcellular fractions. Similar blots were obtained from three other experiments. (**f**) Example images showing Ca^{2+} wave propagation induced by electrical stimulation in the absence (left) and presence (right) of 200 μM GPN (see also Supplementary Information, Movie 4). Top: Differential interference contrast images showing that confluent astrocytes were separated by a cell-free gap created by a scratch with a needle (between the dashed lines). Extracellular stimulation through a microelectrode induced an increase in intracellular Ca^{2+} in the stimulated cell (red arrows) that propagated to astrocytes across the cell-free gap in control cultures (white arrow) but not in GPN-treated cultures. Scale bar, 100 μm. (**g**) Left: Average distance of stimulation-induced Ca^{2+} waves, as illustrated in **f**. Right: Percentage of induced Ca^{2+} waves that propagated across the cell-free gap. The number above each column refers to the total number of cultures examined. Error bars indicate s.e.m. (asterisk, $P < 0.01$ compared with the control group; Student's *t*-test).

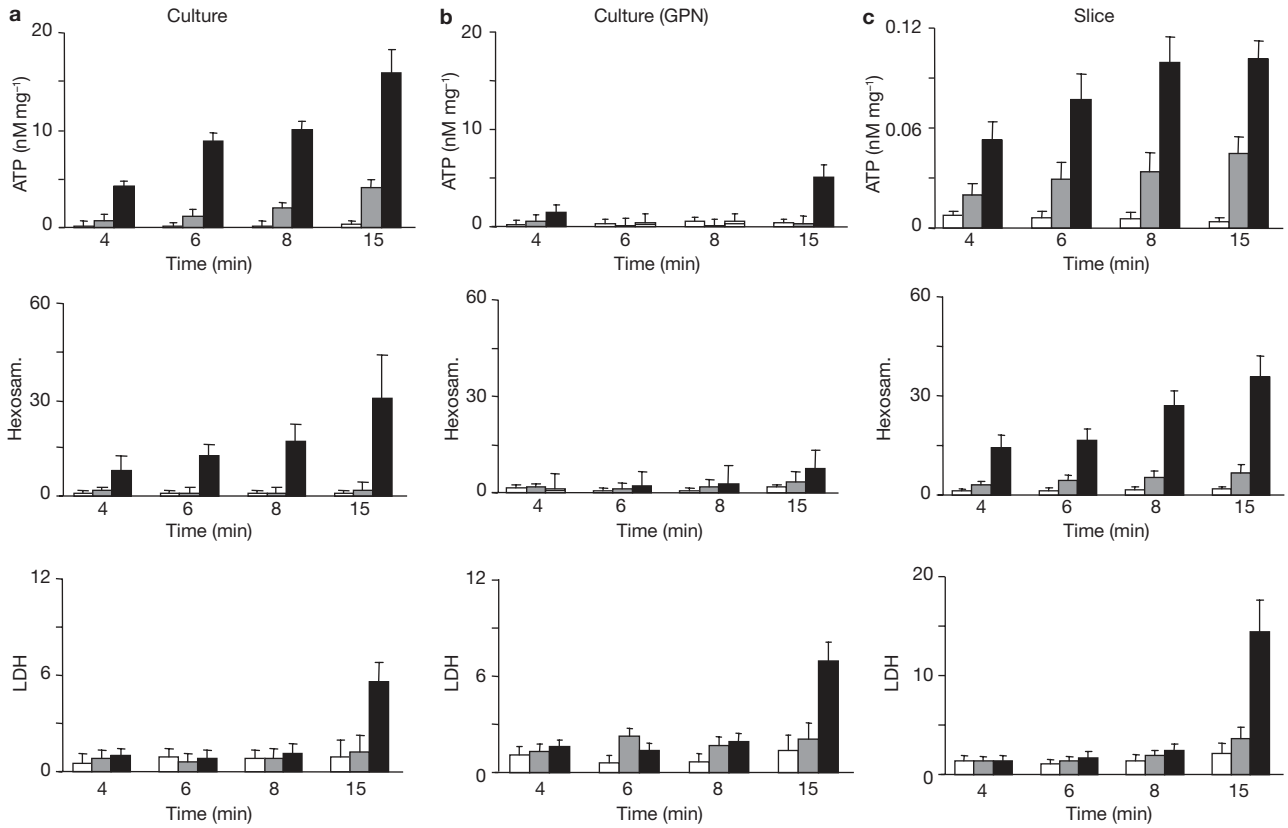

Figure 5 Time course of the release of ATP, β-hexosaminidase (hexosam.) and lactate dehydrogenase (LDH) from cultured astrocytes and hippocampal slices. (**a**, **b**) Release from control cultures (white columns), 1 mM glutamate-treated cultures (grey columns) or 4 mM KCN-treated cultures (black columns), without (**a**) or with (**b**) preincubation with 200 μM GPN. (**c**) Release from control, glutamate-treated or KCN-treated hippocampal slices. Enzyme activities were normalized to the value obtained for the control group. Data represent averaged results from at least six experiments for each group; error bars indicate s.e.m.

used for studying ATP stores and nucleotide-binding proteins[19], labelled the same population of vesicles as those labelled by FM2-10 or CD63–GFP (Fig. 4b–d). Moreover, the treatment with KCN induced a rapid full destaining of the Mant-ATP fluorescence, whereas glutamate induced a slow and partial destaining (Supplementary Information, Fig. S2e, f). To examine further whether lysosomes contain a high level of ATP, we fractionated cultured astrocytes and isolated the lysosomal fraction. As shown in Fig. 4e, of the five fractions only those containing mitochondria (fraction 1, marked by succinate dehydrogenase) and lysosomes (fraction 2, marked by β-hexosaminidase and LAMP1) contained abundant ATP. The high concentration of ATP in these two fractions was detectable only after treatment for 5 min with 1% Triton X-100, indicating that ATP was contained within membrane-enclosed compartments. Furthermore, treatment of these two fractions for 30 min with 200 μM GPN selectively increased the ATP content in the lysosomal fraction (Fig. 4e). Taken together, these results indicate that lysosomes in these cultured astrocytes are enriched in ATP. An ATP peak has previously been found to overlap in sucrose gradients[6] with the secretogranin II immunoreactive fractions obtained from astrocyte cultures, although it is not clear whether these ATP-enriched fractions contain lysosomes.

Further biochemical analysis showed that glutamate induced a time-dependent ATP accumulation in the culture medium, whereas KCN induced the release of much larger amount of ATP, together with the lysosomal enzyme hexosamidase. Hexosamidase release was unlikely to have been caused by KCN-induced cell lysis, at least during the first 8 min of treatment, because during this early stage neither glutamate nor KCN caused significant release of lactate dehydrogenase (Fig. 5a), a usual indicator of cell lysis. In contrast, application of the same concentration of glutamate or KCN for 8 min failed to induce a significant release of ATP or hexosamidase in cultures pretreated with GPN (Fig. 5b), suggesting that lysosomes are indeed the main source of ATP release. A significant release of ATP and hexosamidase was observed 15 min after treatment with KCN in the GPN-pretreated cultures, presumably as a result of cell lysis, as indicated by the elevated release of lactate dehydrogenase. Further experiments showed that similar releases of ATP and hexosamidase were induced in acute hippocampal slices by glutamate and KCN, indicating that lysosome exocytosis may also occur in more intact neural tissues (Fig. 5c).

Lysosomes in melanocytes and in cells derived from the haematopoietic lineage have been termed secretory lysosomes because of their dual functions, namely degradation of proteins and secretion of signalling molecules[7]. Furthermore, lysosomes can fuse with the plasma membrane for membrane repair in response to membrane injury[15]. Our findings that lysosomes in astrocytes contain abundant ATP and have different modes of exocytosis indicate that regulated lysosomal exocytosis in astrocytes may contribute to intercellular signalling. Calcium wave propagation is the most prominent form of intercellular signalling among astrocytes, and this propagation is mediated mainly by ATP release[1–3]. We found that stimulation with an extracellular field that induced a propagating Ca^{2+} wave across a population of astrocytes also

caused a partial destaining of FM2-10-labelled puncta in the stimulated astrocytes (data not shown). In 10 out of 11 experiments, extracellular stimulation evoked Ca^{2+} wave propagation across the cell-free gap in an otherwise confluent astrocyte culture, a reliable indication of ATP-mediated intercellular signalling[1]. In contrast, the same electrical stimulation of GPN-pretreated cultures induced only a localized Ca^{2+} elevation in the stimulated cells in 13 out of 15 experiments (Fig. 4f, g, and Supplementary Information, Movie 4). This inhibition of Ca^{2+} wave propagation by GPN may be attributed to a decrease in ATP release rather than a decrease in the responsiveness of astrocytes to ATP, because Ca^{2+} elevation induced by the perfusion of exogenous ATP was not affected by the pretreatment with GPN (data not shown).

The mechanism underlying ATP accumulation in the lysosome is not clear. Various synaptic and secretory vesicles contain different levels of ATP (ref. 20). Because ATP is negatively charged, proton pump activity that maintains an inside-positive potential of the vesicle membrane is required for the vesicular uptake of ATP by the nucleotide transporter[20]. Putative ATP-binding cassette (ABC) transporters and multidrug-resistant proteins, which can mediate ATP efflux[21,22], are expressed on the lysosomal membrane[23,24]. The high-level activity of the proton pump in the lysosome membrane may maintain an even higher inside-positive membrane potential in the lysosome[25] than that in the synaptic vesicle, allowing lysosomes to accumulate a high concentration of ATP through ABC transporters or multidrug-resistant proteins expressed in the lysosome membrane.

Increases in extracellular ATP (ref. 26) and lysosomal enzymes[13] have been found in ischaemic brain, and the inhibition of lysosomal enzymes has protective effects in preventing ischaemic damage[13]. Our result that disrupting lysosomes prevents the KCN-induced release of ATP as well as lysosomal enzymes (Fig. 5b) suggests that active exocytosis of lysosomes, rather than damage-induced leakage from the cytoplasm, is the major source of increased extracellular ATP and lysosomal enzymes, at least during early stage of ischaemia. Because a high extracellular concentration of ATP may be also toxic to neurons as a result of excessive activation of P2X7 receptors[27], lysosomal ATP release by astrocytes may exacerbate brain injury during ischaemia. Thus, lysosome exocytosis may be a potential therapeutic target for neural protection against ischaemic injury. Furthermore, extracellular nucleotides are known to function as autocrine and paracrine signalling molecules in virtually all tissues and are important in various functions[28]. Our results suggest that regulated lysosome exocytosis may have general functions in other tissues critical for mediating cell–cell communication by releasing ATP in response to physiological as well as pathological stimulation. □

METHODS

All chemicals were from Sigma (St Louis, MO, USA) unless otherwise noted. CD63–GFP plasmid was provided by G. Griffiths (Oxford University, Oxford, UK); wild-type, T22N and Q67L forms of Rab7–GFP were provided by C. Bucci (Lecce University, Italy); NR2B–GFP was provided by J. Luo (Zhejiang University, China). Wild-type and dominant-negative mutant (S34N) forms of Rab5 were provided by G. Li (University of Oklahoma, Oklahoma City, OK, USA). GFP-tagged Rab5 constructs were generated by standard polymerase chain reaction techniques to introduce the desired restriction sites in the flanking sequences of the GFP and Rab5 constructs.

Cell culture and transfection. The use and care of animals followed the guidelines of the Shanghai Institutes for Biological Sciences Animal Research Advisory Committee (Shanghai, China). Primary cultures of astrocytes were prepared as described previously[4]. In brief, astrocytes were prepared from hippocampuses of Sprague–Dawley rats on postnatal day 0, and cultured in minimal essential medium (MEM) with 10% FBS (Gibco). Astrocytes were transfected with plasmid DNA 5 or 6 days after plating, with the calcium phosphate technique (2 mM $CaCl_2$, 3.6 μl; 1 μg/μl DNA, 6 μl; 20.4 μl water; 2 × Hanks balanced salt solution, 30 μl).

Immunostaining. Astrocytes growing on the coverslip were fixed with 4% paraformaldehyde in PBS at 4 °C for 10 min, and permeabilized with 0.01% Triton X-100 in PBS for 12 min before being treated with 10% BSA for 1 h at 25°C. Cultures were then stained with one or two of the following antibodies overnight at 4 °C: mouse anti-LAMP1 (1:500 dilution; Stressgen Biotechnologies), mouse anti-EEA1 (1:150 dilution; BD Transduction Laboratories), rabbit anti-cathepsin D (1:500 dilution), mouse anti-secretogranin II (1:100 dilution; Novocastra Laboratories Ltd), rabbit anti-GFAP (1:1000 dilution; Chemicon, Temecula, CA, USA), mouse anti-VGluT1 anti-VGluT2 (1:200 dilution; Synaptic Systems, Göttingen, Germany). After being washed to remove excess primary antibodies, the cultures were incubated for 1 h at room temperature with fluorescence-conjugated secondary antibodies: anti-mouse IgG-Cy^5, anti-rabbit IgG-Cy^3, or anti-rabbit IgG-Cy^5 (Jackson Immunoresearch, West Grove, PA, USA). Excess antibody was removed and cells were imaged with an Olympus confocal microscope (Olympus Fluoview 500 IX71). In some experiments, astrocytes were loaded with 4 μM AM1-43 for 1 h and washed with quencher solution (0.5 mM 4-sulphonato calix[8]arene, sodium salt (SCAS)) for 4 min at room temperature before fixation for immunostaining.

Fluorescent imaging. Astrocytes were loaded with 4 μM FM1-43, 50 μM FM2-10 or 4 μM AM1-43, a fixable FM1-43 analogue that can be largely preserved after immunochemical procedure[29], in MEM with 10% FBS for more than 2 h and 2 μM Fluo4-AM for 30 min at 37 °C. The astrocytes were then washed for 20 min in extracellular solution (ECS) before transfer to the chamber for imaging under a confocal microscope with a 60× (numerical aperture 1.2; plan-Apochromat) water-immersion objective. The time courses of the changes in fluorescence of FM1-43 or FM2-10 were obtained at an image interval of 5 s with $\lambda_{emission} > 560$ nm and $\lambda_{excitation} = 488$ nm. A low laser power (less than 0.5% power) was used to avoid possible fluorescent bleaching. The decrease in fluorescence intensities of FM due to photobleaching was less than 5% over 10 min. In some experiments, astrocytes were transfected with EGFP-linked molecules and the fluorescence was detected at 505–525 nm with excitation at 488 nm. For combined FM dye and Ca^{2+} imaging, astrocytes were preloaded with 2 μM Fluo-4 AM for 30 min before being loaded with FM. In some experiments, astrocytes were incubated with 300 μM MANT-ATP for 5–8 h in MEM with 10% FBS, and fluorescence was detected at 430–480 nm with excitation at 364 nm. Data analysis was performed with Metamorph software (Universal Imaging Corp., Downington, PA) and Fluoview 500 software (Olympus MicroImaging, Inc.).

Extracellular ATP measurements. The concentration of extracellular ATP was quantified with a bioluminescence method using the luciferase–luciferin test as described previously[4]. In brief, the culture medium of astrocytes or incubation medium for slices was replaced with recording medium. The ectonucleotidase inhibitor dipyridamole (10 μM) was added into the extracellular solution throughout the experiment to decrease ATP hydrolysis[4]. Glutamate or KCN was added to the medium, and supernatant was collected at 4, 6, 8 and 15 min after stimuli. A 50-μl sample was added to 50 μl of ATP assay mix containing luciferase–luciferin buffer. Luminescence was measured with a V3.1 Sirius luminometer (Berthold Detection Systems). A calibration curve was obtained from standard ATP samples and the luminescence of the recording medium was measured as the background. For measurement of ATP content in different subcellular fractions derived from centrifugation, 1% Triton X-100 was added for 5 min before the ATP assay to destroy organelle membranes.

TIRFM. Imaging and analysis for TIRFM were performed as described previously[16,30]. An objective-type TIRF microscope was used to observe the FM dye-loaded astrocytes grown on a high-refractive-index glass coverslip. The setup consisted of an argon-ion laser (488 nm), a high-numerical-aperture (NA) oil-immersion objective (100×, 1.65 NA), an inverted microscope (IX71; Olympus, Tokyo, Japan) and a cool-charge-coupled-device camera (pixel size 6.7 μm; PCO SensiCam; PCO, Kelheim, Germany). Images were acquired by TILL Vision software (TILL Photonics, Gräfelfing, GERMANY) and analysed with IPP5.0 (Imaging

Pro Plus). For measurement of fluorescence intensity, a region of interest (ROI) was drawn around the puncta and the average intensity was measured in this region. The intensity of the concentric annulus around the ROI (puncta) with a diameter of 2.5 times that of the ROI was also measured.

Statistical analysis. Data are presented as mean ± s.e.m. Statistical comparisons were assessed with an analysis of variance or Student's *t*-test; $P < 0.05$ was taken as significant.

Note: Supplementary Information is available on the Nature Cell Biology website.

ACKNOWLEDGEMENTS

We thank M-m. Poo for critical comments on the manuscript, and Z. Zhou, X. K. Chen and Y. Zhou for valuable discussion. This work was supported by grants from the Major State Basic Research Program of China (G200077800 and 2006CB806600) and the National Natural Science Foundation of China (30321002).

COMPETING FINANCIAL INTERESTS

The authors declare no competing financial interests.

Published online at http://www.nature.com/naturecellbiology/
Reprints and permissions information is available online at http://npg.nature.com/reprintsandpermissions/

1. Guthrie, P. B. *et al.* ATP released from astrocytes mediates glial calcium waves. *J. Neurosci.* **19,** 520–528 (1999).
2. Haydon P. G. & Carmignoto, G. Astrocyte control of synaptic transmission and neurovascular coupling. *Physiol. Rev.* **86,** 1009–1031 (2006).
3. Cotrina, M. L., Lin, J. H., Lopez-Garcia, J. C., Naus, C. C. & Nedergaard, M. ATP-mediated glia signaling. *J. Neurosci.* **20,** 2835–2844 (2000).
4. Zhang, J. M. *et al.* ATP released by astrocytes mediates glutamatergic activity-dependent heterosynaptic suppression. *Neuron* **40,** 971–982 (2003).
5. Pascual, O. *et al.* Astrocytic purinergic signaling coordinates synaptic networks. *Science* **310,** 113–116 (2005).
6. Coco, S. *et al.* Storage and release of ATP from astrocytes in culture. *J. Biol. Chem.* **278,** 1354–1362 (2003).
7. Blott, E. J. & Griffiths, G. M. Secretory lysosomes. *Nature Rev. Mol. Cell Biol.* **3,** 122–131 (2002).
8. Gardella, S. *et al.* $CD8^+$ T lymphocytes induce polarized exocytosis of secretory lysosomes by dendritic cells with release of interleukin-1β and cathepsin D. *Blood* **98,** 2152–2159 (2001).
9. Jadot, M., Colmant, C., Wattiaux-De, C. S. & Wattiaux, R. Intralysosomal hydrolysis of glycyl-L-phenylalanine 2-naphthylamide. *Biochem. J.* **219,** 965–970 (1984).
10. Klingauf, J., Kavalali, E. T. & Tsien, R. W. Kinetics and regulation of fast endocytosis at hippocampal synapses. *Nature* **394,** 581–585 (1998).
11. Rizzoli, S. O., Richards, D. A. & Betz, W. J. Monitoring synaptic vesicle recycling in frog motor nerve terminals with FM dyes. *J. Neurocytol.* **32,** 539–549 (2003).
12. Harata, N. C., Choi, S., Pyle, J. L., Aravanis, A. M. & Tsien, R. W. Frequency-dependent kinetics and prevalence of kiss-and-run and reuse at hippocampal synapses studied with novel quenching methods. *Neuron* **49,** 243–256 (2006).
13. Hayashi, T., Shoji, M. & Abe, K. Molecular mechanisms of ischemic neuronal cell death—with relevance to Alzheimer's disease. *Curr. Alzheimer Res.* **3,** 351–358 (2006).
14. Dubinsky, J. M. & Rothman, S. M. Extracellular calcium concentration during 'chemical hypoxia' and excitatoric neuronal injury. *J. Neurosci.* **11,** 2545–2552 (1991).
15. Reddy, A., Caler, E. V. & Andrews, N. W. Plasma membrane repair is mediated by Ca^{2+}-regulated exocytosis of lysosomes. *Cell* **106,** 157–169 (2001).
16. Jaiswal, J. K., Chakrabarti, S., Andrews, N. W. & Simon, S. M. Synaptotagmin VII restricts fusion pore expansion during lysosomal exocytosis. *PLoS Biol.* **2**, E233 (2004).
17. Heidemann, A. C., Schipke, C. G. & Kettenmann, H. Extracellular application of nicotinic acid adenine dinucleotide phosphate induces Ca^{2+} signaling in astrocytes in situ. *J. Biol. Chem.* **280,** 35630–35640 (2005).
18. Chen, X., Wang, L., Zhou, Y., Zheng, L. H. & Zhou, Z. 'Kiss-and-run' glutamate secretion in cultured and freshly isolated rat hippocampal astrocytes. *J. Neurosci.* **25,** 9236–9243 (2005).
19. Sorensen, C. E. & Novak, I. Visualization of ATP release in pancreatic acini in response to cholinergic stimulus. Use of fluorescent probes and confocal microscopy. *J. Biol. Chem.* **276,** 32925–32932 (2001).
20. Sperlagh, B. & Vizi, S. E. Neuronal synthesis, storage and release of ATP. *Semin. Neurosci.* **8,** 175–186 (1996).
21. Ballerini, P. *et al.* Glial cells express multiple ATP binding cassette proteins which are involved in ATP release. *NeuroReport* **13,** 1789–1792 (2002).
22. Abraham, E. H. *et al.* The multidrug resistance (*mdr1*) gene product functions as an ATP channel. *Proc. Natl Acad. Sci. USA* **90,** 312–316 (1993).
23. Eskelinen, E. L., Tanaka, Y. & Saftig, P. At the acidic edge: emerging functions for lysosomal membrane proteins. *Trends Cell Biol.* **13,** 137–145 (2003).
24. Cabrita, M. A., Hobman, T. C., Hogue, D. L., King, K. M. & Cass, C. E. Mouse transporter protein, a membrane protein that regulates cellular multidrug resistance, is localized to lysosomes. *Cancer Res.* **59,** 4890–4897 (1999).
25. Harikumar, P. & Reeves, J. P. The lysosomal proton pump is electrogenic. *J. Biol. Chem.* **258,** 10403–10410 (1983).
26. Parkinson, F. E. & Xiong, W. Stimulus- and cell-type-specific release of purines in cultured rat forebrain astrocytes and neurons. *J. Neurochem.* **88,** 1305–1312 (2004).
27. Duan, S. & Neary, J. P2X7/P2Z receptors: properties and relevance to CNS functions. *Glia* **54**,738–746 (2006).
28. Brake, A. J. & Julius, D. Signaling by extracellular nucleotides. *Annu. Rev. Cell Dev. Biol.* **12,** 519–541 (1996).
29. Renger, J. J., Egles, C. & Liu, G. A developmental switch in neurotransmitter flux enhances synaptic efficacy by affecting AMPA receptor activation. *Neuron* **29,** 469–484 (2001).
30. Jaiswal, J. K., Andrews, N. W. & Simon, S. M. Membrane proximal lysosomes are the major vesicles responsible for calcium-dependent exocytosis in nonsecretory cells. *J. Cell Biol.* **159,** 625–635 (2002).

nature cell biology

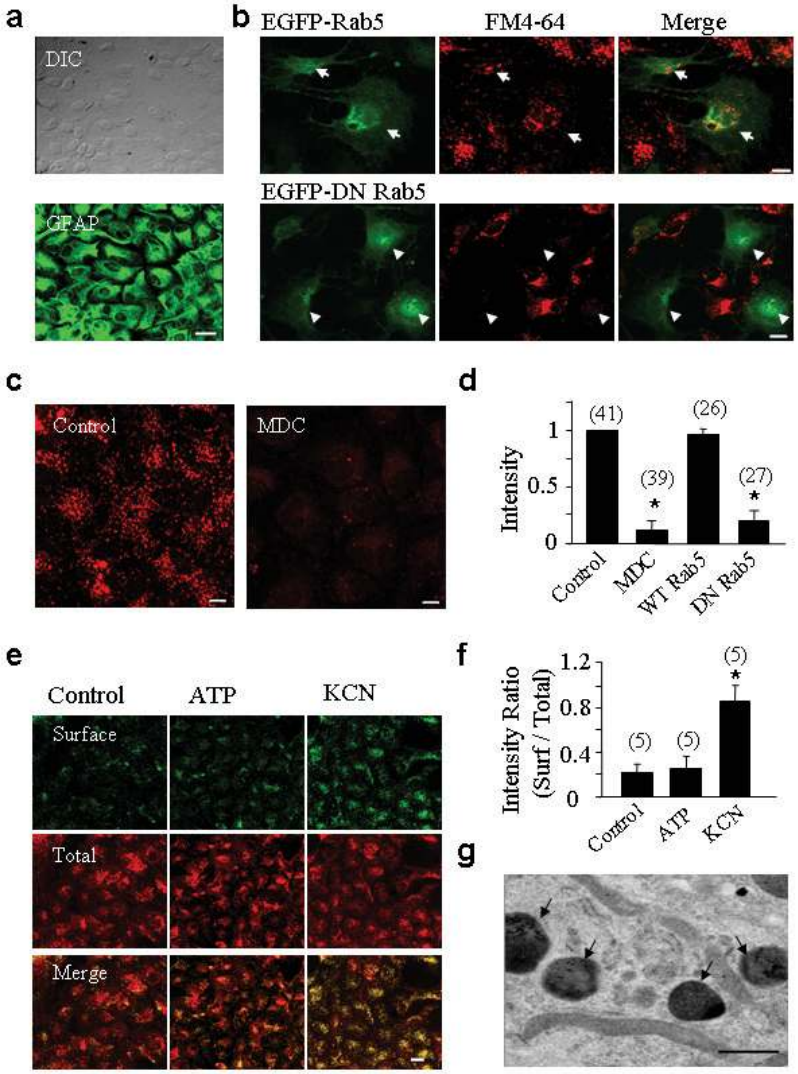

Figure S1. FM dyes were loaded into astrocytes through the endocytotic pathway. **(a)** Purified astrocytes were immunostained with anti-GFAP (green) and observed under DIC (upper panel) and fluorescent microscope (lower panel). **(b)** The FM4-64-labeled puncta were largely prevented in cells transfected with EGFP-linked dominant negative Rab 5 (EGFP-S34N Rab 5; indicated by arrowheads in the lower panels), but not in cells transfected with wild type Rab 5 (EGFP-Rab 5, indicated by arrows in upper panels), a small G protein that plays a key role in biogenesis of early endosomes from endocytosis[1]. **(c)** The FM2-10-labeled puncta were largely prevented in the presence of 200 M MDC (right panel), an inhibitor of the endocytosis[2]. Bars in **a** to **c**, 10 m. **(d)** Averaged fluorescence intensity of FM dyes in astrocytes under various conditions as shown in **a** and **c**. Data were normalized with averaged fluorescence intensity of the FM dye detected in control cells (without MDC treatment or transfection). The number associated with each column refers to the number of cells examined. "*" $p<0.01$, as compared with control group. **(e)** Immunostaining of astrocytes with anti-LAMP1 that recognizes the luminal N-terminal domain of LAMP1 before permeabilizing the cells with methanol shows the surface presence of LAMP1 (surface, green), whereas the second immunostaining of the cells after permeabilization reveals the cytoplasmic and surface LAMP1 (total, red). Note significantly increased surface staining in KCN-(right column), but not ATP-(middle column) treated cultures. **(f)** Summary data showing the ratio of surface/total anti-LAMP1 staining in different treated cultures as shown in **e**. Error bars in **d** and **f** represent s.e.m. ("*" $p<0.01$, as compared with the control group, Student's *t* test).The number associated with each column refers to the number of experiments examined for each condition. **(g)** Example EM of the photoconverted FM1-43 precipitates in cultured astrocytes. Arrows indicate labeled lysosomes. Scale bars, 10 m for **e** and 0.5 m for **g**.

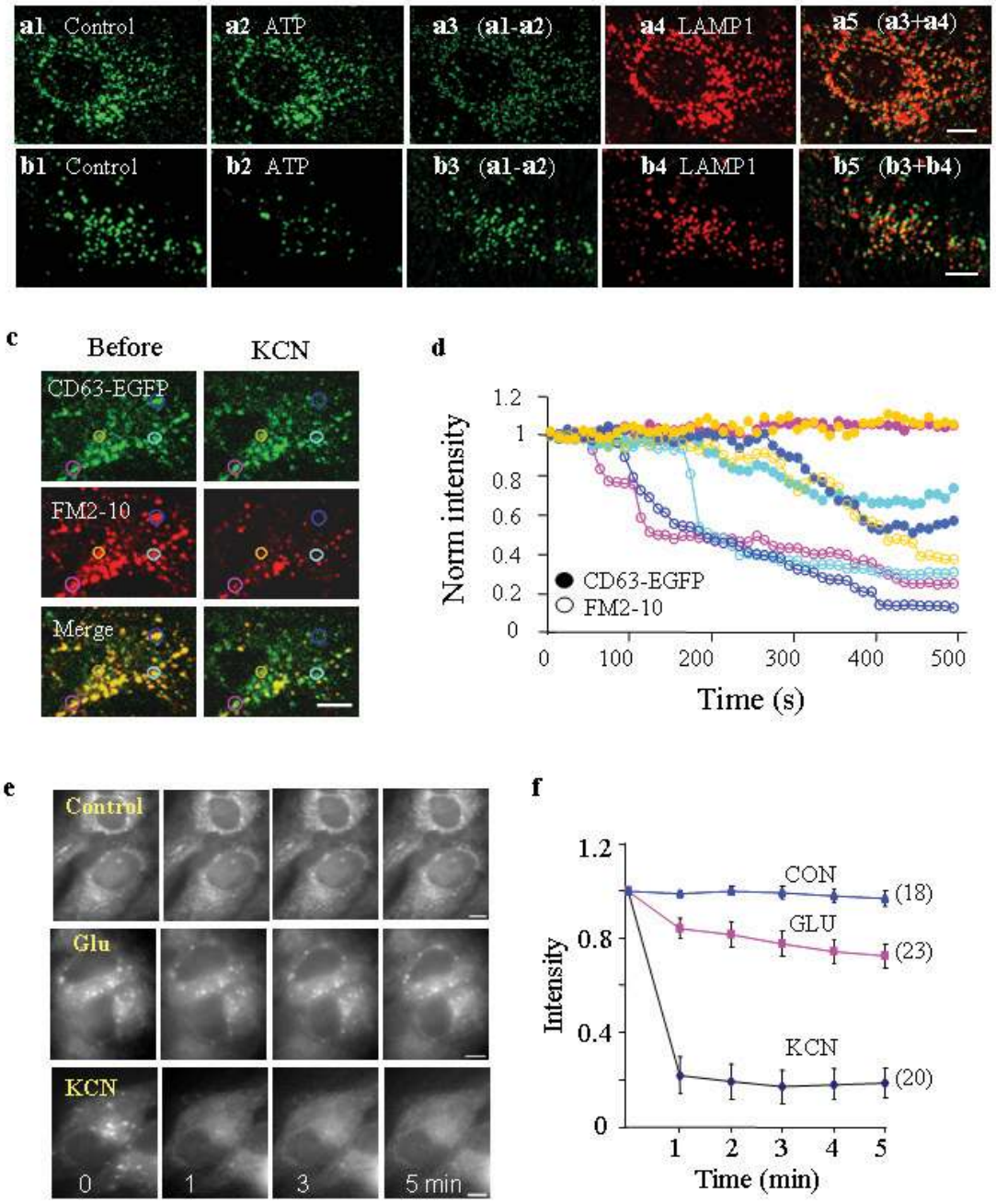

Figure S2 Example images of ATP- or KCN-induced destaining of FM dye- and Mant-ATP-labeled puncta in lysosomes. (**a**) and (**b**) Example confocal images of FM2-10-labeled puncta before (**a1** and **b1**) and during perfusion of 1 mM ATP (**a2**) or 4 mM KCN (**b2**). Puncta exhibiting partial or full destaining shown in (**a3**) and (**b3**) were obtained by subtracting (**a2**) and (**b2**) from (**a1**) and (**b1**) respectively. These cells were then immunostained with anti-LAMP1 (**a4** and **b4**). (**a5**) and (**b5**) are merged images from **a3**, **a4** with **b3**, **b4** respectively, showing that most destained (either partial or full) puncta are LAMP1 positive. (**c**) Example images of puncta co-labeled with GFP-linked CD-63 (green) and FM2-10 dye (red) before (control, left panels) and after (right panels) 4 mM KCN treatment. Merged images (bottom panels) show more green puncta after KCN treatment. (**d**) Example time course of KCN-induced destaining of punta shown in **c**. Lines in different colors correspond to the imaged puncta in **c** marked by the circles of the same color, with filled symbols for FM2-10 signal and opened symbols for CD63-GFP. Note that slower and less destaining of CD63-GFP signaling than that of FM2-10 signaling (see also Movie 1). **(e)** Confocal images showing time course of glutamate- (middle panels) and KCN- (bottom panels) induced MANT-ATP destaining. Glutamate or KCN was added at 30 s (between the first and second images). Scale bars, 10 m. (**f**) Summarized time course of glutamate- and KCN- induced destaining of MANT-ATP puncta shown in **e**. Data were normalized by the average fluorescence intensity obtained before the glutamate or KCN application. The number associated with each line refers to the number of cells examined for each condition.

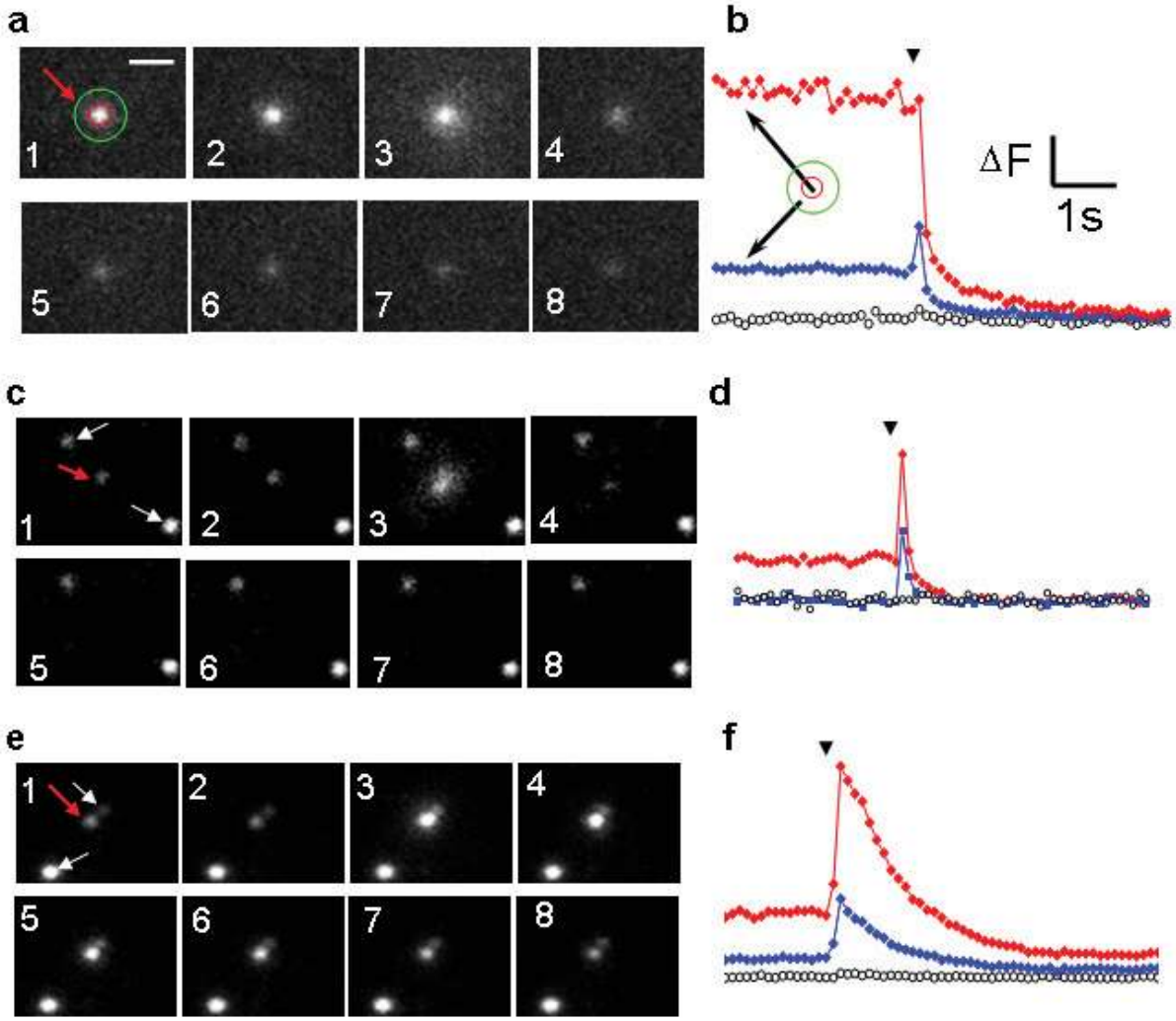

Figure S3. Examples of single lysosome (labeled by FM2-10) exocytosis revealed by TIRF imaging (see also Movie 2). (**a**) Sequential images of a "pre-docked" lysosome (indicated by the red arrow in the left panel) exhibiting full exocytosis during KCN treatment. Numbers associated with each panel indicate sequential imaging order with an interval of 100 ms. Note the diffuse cloud of the FM2-10 fluorescence showed in the third panel, a characteristic of vesicle fusion. (**b**) Time course of the fluorescence changes in the puncta shown in **a**. Red and blue symbols represent fluorescence intensity measured at the puncta and concentric annulus around the puncta, as indicated by the red and green circles respectively in the left panel in **a**. Black symbols represent the background brightness in the puncta-free region. The complete exocytosis of this "pre-docked" lysosome is characterized by the rapid spread of fluorescence (increased fluorescence intensity at the concentric annulus), followed by disappearance of the puncta due to FM2-10 dye defusing away. (**c**) and (**d**) Sequential images (**c**) and time course of fluorescence changes (**d**) of a less pre-docked lysosome (indicated by the red arrow in **c**) exhibiting full exocytosis during KCN treatment. Note the transient increased fluorescence in both central region and surrounding annulus (the third panel in **c**) of the puncta followed by disappearance of the puncta. (**e**) and (**f**) Example images (**e**) and the time course of fluorescence changes (**f**) in a punctum (indicated by the red arrow in **e**) exhibiting partial exocytosis in the presence of 1 mM ATP.

Movie 1. KCN-induced differential destaining of fluorescence signals in puncta labeled by FM2-10 (red) and CD63-GFP (green) , indicating that lysosome membrane was restricted from diffusing into plasma membrane. KCN was added at 0 sec.

Movie 2. Examples of single punctum exocytosis revealed by TIRF. Left (KCN-induced complete fusion of an "old puncta"), middle (KCN-induced complete fusion of a "new puncta"), and right (ATP-induced partial exocytosis), from same imaging fields as shown in Figure S3a, S3c, and S3e, respectively.

Movie 3. KCN-induced exocytosis of FM2-10-labeled puncta revealed by TIRFM. Note the emerging "new puncta" after KCN application.

Movie 4. Calcium wave propagation induced by electrical stimulation (at 0 sec) in cultured astrocytes with (right) or without (left) GPN treatment (see also Fig. 4**f**).